Original Article

MOLECULAR METABOLISM

# CPT1C deficiency in SF1 neurons impairs early metabolic adaptation to dietary fats, leading to obesity

A. Fosch[1,6], D.S. Pizarro[1,6], S. Zagmutt[1], A.C. Reguera[1], G. Batallé[1], M. Rodríguez-García[1], J. García-Chica[1], O. Freire-Agulleiro[2], C. Miralpeix[1,3], P. Zizzari[3], D. Serra[4,5], L. Herrero[4,5], M. López[2,5], D. Cota[3], R. Rodríguez-Rodríguez[1,5,*], N. Casals[1,5,**]

## ABSTRACT

**Objectives:** SF1 neurons of the ventromedial hypothalamus (VMH) play a pivotal role in regulating body weight and adiposity, particularly in response to a high-fat diet (HFD), as well as in the recovery from insulin-induced hypoglycemia. While the brain-specific CPT1C isoform is well known for its role in controlling food intake and energy homeostasis, its function within specific hypothalamic neuronal populations remains largely unexplored. Here, we explore the role of CPT1C in SF1 neurons.

**Methods:** Mice deficient in CPT1C within SF1 neurons were generated, and their response to a HFD was investigated.

**Results:** SF1-*Cpt1c*-KO mice fail to adjust their caloric intake during initial HFD exposure, which is associated with impaired activation of the melanocortin system. Furthermore, these mice exhibit disrupted metabolic gene expression in the liver, muscle, and adipose tissue, leading to increased adiposity independently of food intake. In contrast, their response to glucose or insulin challenges remains intact. After long-term HFD exposure, SF1-Cpt1c-KO mice are more prone to developing obesity and glucose intolerance than control littermates, with males exhibiting a more severe phenotype. Interestingly, CPT1C deficiency in SF1 neurons also results in elevated hypothalamic endocannabinoid (eCB) levels under both chow and HFD conditions. We propose that this sustained eCB elevation reduces VMH activation by fatty acids and impairs the SF1-POMC drive upon fat intake.

**Conclusion:** Our findings establish CPT1C in SF1 neurons as essential for VMH-driven dietary fat sensing, satiety, and lipid metabolic adaptation.



**Keywords** CPT1C; SF1 neurons; High-fat diet; Endocannabinoids; Adiposity; Food intake

## 1. INTRODUCTION

The central regulation of body weight is a complex process that involves intricate neural circuits within the hypothalamic nuclei and extra-hypothalamic areas, orchestrating appetite and energy homeostasis. The ventromedial nucleus of the hypothalamus (VMH), recognized not only as a satiety center but also as a crucial regulator of energy balance, influences brown fat thermogenesis, peripheral lipid metabolism and glucose homeostasis [1]. Electric stimulation of the VMH triggers hypophagia and energy expenditure (EE), and a decrease in respiratory exchange ratio (RER), indicating a preference for fats over glucose as the primary energy substrate to supply the cellular oxidation rate [2].

The majority of VMH neurons, particularly those in the dorsomedial and central regions of the VMH, express the nuclear receptor steroidogenic factor 1 (SF1), a transcription factor encoded by *Nr5a1* gene, specific to this nucleus and essential for its development and function [3—5]. Optogenetic and chemogenetic studies have revealed that SF1-positive cells are responsible for most of the intrinsic actions of the VMH, including satiety signaling, promotion of EE, facilitation of fat mobilization [6,7], and recovery from insulin-induced hypoglycemia [8]. Interestingly, transgenic mice with impaired expression of several molecular targets in SF1 neurons often display altered metabolic phenotypes, particularly under exposure to a high-fat diet (HFD), but not when fed regular chow, emphasizing a role for SF1 neurons in

[1]Department of Biomedical Sciences, Faculty of Medicine and Health Sciences, Universitat Internacional de Catalunya, 08195 Sant Cugat del Vallès, Spain [2]Department of Physiology, CIMUS, University of Santiago de Compostela-Instituto de Investigación Sanitaria, Santiago de Compostela, 15782, Spain [3]INSERM, Neurocentre Magendie, U1215, University of Bordeaux, 3300 Bordeaux, France [4]Department of Biochemistry and Physiology, School of Pharmacy and Food Sciences, Institut de Biomedicina de la Universitat de Barcelona (IBUB), Universitat de Barcelona, Barcelona, 08028 Spain [5]Centro de Investigación Biomédica en Red de Fisiopatología de la Obesidad y la Nutrición (CIBEROBN), Instituto de Salud Carlos III, 28029 Madrid, Spain

[6] Fosch A and Pizarro DS contributed equally to this work.

*Corresponding author. Centro de Investigación Biomédica en Red de Fisiopatología de la Obesidad y la Nutrición (CIBEROBN), Instituto de Salud Carlos III, 28029 Madrid, Spain. E-mail: rrodriguez@uic.es (R. Rodríguez-Rodríguez).

**Corresponding author. Centro de Investigación Biomédica en Red de Fisiopatología de la Obesidad y la Nutrición (CIBEROBN), Instituto de Salud Carlos III, 28029 Madrid, Spain. E-mail: ncasals@uic.es (N. Casals).

Received February 6, 2025 • Revision received April 14, 2025 • Accepted April 16, 2025 • Available online 21 April 2025

https://doi.org/10.1016/j.molmet.2025.102155

  

metabolic adaptation to increased fat consumption [1]. Moreover, recent data suggest that unsaturated fats, but not saturated ones, activate SF1 neurons driving satiety and EE [9]. However, the molecular mechanisms and neural circuitry that underlie the sensing of fats by SF1 neurons remain poorly understood. Notably, the endocannabinoid (eCB) receptor CB1, which is highly expressed in SF1 neurons [10] decreases the excitability of those neurons and modulates feeding and fuel selection by peripheral tissues based on the type of diet [10,11].

The neuron-specific carnitine palmitoyltransferase 1C (CPT1C), has emerged as a key player in appetite regulation and nutrient partitioning in the hypothalamus, including the VMH [12,13]. Global CPT1C knockout (KO) mice exhibit impaired feeding responses to leptin and ghrelin [14,15], and disrupted diet-induced brown fat thermogenesis, making them more susceptible to become obese when fed a HFD [16]. Moreover, CPT1C is involved in food preference [17], fuel selection under fasting conditions [18], and the sensing of fats by the hypothalamus [9]. However, there is limited data regarding the role of CPT1C in specific nuclei of the hypothalamus. At the molecular level, CPT1C, which is unique in lacking enzymatic activity within the CPT1 family [19], functions as a nutrient sensor by binding malonyl-CoA within neurons [20–26]. Malonyl-CoA is a lipid metabolite that dynamically fluctuates in the hypothalamus based on the nutritional state [27,28] and regulates feeding behavior and energy homeostasis [29–37]. Our recent studies indicate that CPT1C regulates AMPA receptor trafficking and synaptic transmission through malonyl-CoA [22,38,39]. In addition, CPT1C interacts with the eCB hydrolase $\alpha/\beta$-hydrolase domain-containing 6 (ABHD6), modulating its enzymatic activity depending on nutrients and malonyl-CoA availability [26]. Considering the existing evidence, we postulated that CPT1C in SF1 plays a significant role in mediating the response to dietary lipids. Our findings demonstrate that the specific deletion of *Cpt1c* in SF1 neurons diminishes the responsiveness of SF1 neurons to fats, increases levels of eCB, and blunts $\alpha$-MSH levels. This cascade of events results in impaired satiety signaling, disrupted nutrient partitioning, and an increased propensity for obesity. These observations elucidate a novel mechanism linking CPT1C function in SF1 neurons to energy homeostasis and body weight regulation.

## 2. METHODS

### 2.1. Animals

Male and female mice were housed on 12 h/12 h light/dark cycle (light on at 8 am, light off 8 pm) in a temperature- and humidity-controlled room. Animals were group housed and allowed free access to water and standard laboratory chow diet, otherwise indicated. Animals used for experimentation were between 8 and 12 weeks of age at the starting point of the experiments. All animal procedures were performed in agreement with European guidelines (2010/63/EU) and approved by the Ethical Committee of the University of Barcelona (n. 10906 and n. 10210 from the Generalitat de Catalunya) and of the University of Bordeaux (n. 30252). All efforts were made to minimize animal suffering and to minimize the number of animals used. Animal studies are reported in compliance with the ARRIVE guidelines.

### 2.2. Generation of SF1-Cpt1c-KO mice

Mice deficient of CPT1C in SF1 neurons were generated through two consecutive steps using Flp-FRT and Cre-loxP technologies at CBATEG from Universitat Autònoma de Barcelona. Sperm of the strain C57BL/6N-CPT1c$^{tm1a(EUCOMM)Wtsi}$, containing exons 4 to 6 of *Cpt1c* flanked by two LoxP sequences, a lacZ cassette and a *neo* gene, was obtained from KOMP Repository (University of California, Davis). This sperm was used for an *in vitro* fertilization to generate heterozygous mice called KO-first. LacZ and Neo cassettes were deleted by breeding KO-first with mice containing FlpO in heterozygosis (FlpO mice) from the Mouse Mutant Core Facility (MMCF) of IRB Barcelona, to get a *Cpt1c*$^{loxP/-}$ mice. These animals were bred with SF1-Cre mice (Tg(Nr5a1-cre)Lowl/J, stock number 012462 from The Jackson Laboratory, Bar Harbor, ME) to generate SF1-Cre;*Cpt1c*$^{loxP/-}$, which finally were bred with a homozygous *Cpt1c*$^{loxP/loxP}$ mice to get SF1-Cre;*Cpt1c*$^{loxP/loxP}$, also called SF1-*Cpt1c*-KO. *CPT1c*$^{loxP/loxP}$ mice resulting from this last breeding were control littermates called SF1-*Cpt1c*-WT mice.

### 2.3. Genotyping

DNA from VMH or ear punches were used for genotyping. VMH samples were collected using a brain matrix and stored at −80 °C until used. DNA was obtained using Proteinase K (3115887001, Roche, Basel, Switzerland) digestion followed by phenol-chloroform extraction and ethanol precipitation. DNA from ear punches was extracted with 50 mM NaOH and buffered in TRIS 1M pH 8. The oligonucleotide enhancers used for DNA amplification are described in Supplemental Table 1 and Supplemental Fig. 1.

### 2.4. Administration of high fat diets

Mice were fed a HFD (60% kcal from fat, ref. D12492) or a standard diet (SD, 10% kcal from fat, ref. D12450J, Research Diets, New Brunswick, USA) for 5 days or 8 weeks. During this period, body weight and the amount of each diet eaten was weakly measured. At the end of the study, mice were sacrificed by cervical dislocation and hypothalamus, epididymal white adipose tissue (eWAT), subcutaneous WAT (sWAT), brown adipose tissue (BAT), liver and soleus muscle were collected and stored at −80 °C until further processing.

For the analysis of neuronal activation by c-Fos, mice were fasted for 3 h during the light phase followed by a refeeding period of 2 h with HFD or SD. Then, mice were perfused for brain cryopreservation.

For the pair-feeding experiment mice were housed in cages equipped with automatic feeders (SmartWaiters, Cibertec, Madrid, Spain). Mice were acclimatized for a week with *ad libitum* SD. Then, the feeders were programmed to stay open for 1 h before the onset of the light phase and 1 h previous to the dark phase for one week. Food Intake was recorded during this period and mean caloric intake of SD was calculated. Calories were equated between SD and HFD, and feeders were programmed to allow the mice to eat 0.8 g of HFD both at the onset of light and dark phases for five days. After each mouse had eaten 0.8 g of HFD the feeder would automatically close. Mice body weight was recorded at the beginning and end of the experiment. Tissues were collected as previously described.

### 2.5. Intracerebroventricular (ICV) cannulation surgery and oleic acid administration

Mice were anesthetized with 75 mg/kg of ketamine (Ketamidor® 100 mg/mL Richter Pharma AG, Bagres Austria) and 10 mg/kg of xylazine (Rompun® 20 mg/mL Bayer, Leverkusen, Germany). Cannulas were stereotaxically implanted into the lateral cerebral ventricle, being the coordinates 0.58 mm posterior to Bregma, 1 mm lateral to the midsagittal suture and 2.2 mm of depth. Mice were individually caged and allowed to recover for at least 5 days before the experiment. Cannula placement was verified by a positive dipsogenic response to angiotensin II (1 nmol in 1 mL; Sigma–Aldrich, Saint Louise, USA).

Oleic acid (03880; Sigma–Aldrich, St Louis, USA) or vehicle were injected into ICV-cannulated mice. Oleic acid was complexed with

 

fresh 40 % HPB (2-Hydroxypropyl)-β-cyclodextrin (H107 Sigma—Aldrich, St Louis, USA). 9 nmols of oleic acid/dose and 2 μL/dose were injected. Animals did not have access to food during the whole procedure. After 2 h, mice were perfused for brain collection, as indicated below.

### 2.6. Administration of adeno-associated virus (AAVs) within the VMH

For the stereotaxic surgery, mice were anesthetized as previously described. Stereotaxic surgery to target VMH was carried out with the following coordinates: 1.5 mm posterior from Bregma, ±0.5 mm lateral to midline and 5.8 mm deep. Purified AAVs expressing mCherry under Cre activity (AAV-CRE-mCherry) [40] were injected bilaterally over 10 min through a 33-gauge injector connected to a 5 μL Hamilton® Syringe (65460-02, Hamilton Company, Reno, USA) and an infusion pump. 0,4 nL with a viral titer of $1{,}23 \times 10^{12}$ pfu/mL were infused in each injection site. After surgery, an analgesic solution (Meloxidyl® 5 mg/mL, Ceva Santé Animale, Libourne, France) was subcutaneously administered to a final dose of 1 mg/kg of body weight. During the first two days of recovery, the analgesic was administered through the drinking water with a final solution of 5 mg/L. Mice underwent 3 weeks of recovery before their use for the study.

### 2.7. Indirect calorimetry, in cage-locomotor activity and gas exchange analysis

Indirect calorimetry, in-cage locomotor activity and gas exchange analysis were carried out in light, temperature and humidity controlled calorimetric chambers (TSE Systems GmbH, Moos, Germany) as described previously [41]. The light cycle was 12 h/12 h light/dark phase (lights on 3am, lights off 3pm) at 22 °C. Mice were acclimated for 5 days before recording. $O_2$ consumption and $CO_2$ production were measured to calculate RER (or respiratory quotient, RQ) and EE. Locomotor activity was determined using an infrared light beam system. All measurements were taken every 20 min.

### 2.8. Magnetic resonance imaging (MRI)

Body composition analysis of SF1-*Cpt1c*-WT and SF1-*Cpt1c*-KO mice was performed by nuclear echo magnetic resonance imaging (EchoMRI 900; EchoMedical Systems, New York, USA) to evaluate the total amount of fat and lean mass of mice. Mice were weighted and placed into a movement restrainer before going inside the EchoMRI. The analysis was performed previously to HFD exposition and after the 5-day and the 8-week exposure to HFD. All measurements were taken in duplicates.

### 2.9. Glucose and insulin tolerance tests

All glucose measurements were performed using the glucometer Aviva from Accu-Chek® (Roche, Basel, Switzerland) and test strips (06453970, Roche, Basel, Switzerland) on the second drop after a little cut on the tail. Glucose tolerance test (GTT) and insulin tolerance test (ITT) were conducted in 6 h fasted mice, starting at the beginning of the light phase. 20 % glucose (Glucose 20 % B. Braun Medical, Melsungen, Germany) was injected intraperitoneally with a final dose of 2 g/kg body weight. 0.1 IU/mL of human insulin (Humulin 100 IU/mL, Lilly Medical, Indianapolis, USA) was injected with a final dose of 0.5 IU/kg body weight. Data were represented as glycaemia evolution over time and area under the curve. Glucose disappearance rate ($K_{ITT}$) was calculated using the first 30 min.

### 2.10. RNA preparation and quantitative RT-PCR

Total RNA was extracted from tissues using Trizol Reagent (Fisher Scientific, Madrid, Spain). Quantitative RT-PCR analysis was performed as previously described [9]. SsoAdvanced™ SYBR®Green Supermix (172-5261, BioRad, Hercules, USA) was used for double-stranded DNA intercalating agents and SsoFast™ Probes Supermix (172-5231, BioRad, Hercules, USA) for TaqMan assay. SYBR Green assay primers are listed in Supplemental Table 2. Taqman Gene Expression assay primers for *Ucp1* were used (for: 5′-CACACCTC-CAGTCATTAAGCC, and rev: 5′-CAAATCAGCTTTGCCTCACTC). All primers were from IDT DNA Technologies, Leuven, Belgium. Relative mRNA levels were measured using the CFX96 Real-time System, C1000 Thermal Cycler (BioRad, CA, USA). Relative gene expression was estimated using the comparative Ct ($2^{-\Delta\Delta Ct}$) method in comparation to *Gapdh* levels.

### 2.11. Western blotting

Western blot was performed as previously described [9]. Briefly, soleus muscle was homogenized in RIPA buffer (Sigma—Aldrich, Madrid, Spain) containing protease and phosphatase inhibitor cocktails. Protein extracts were separated on SDS-PAGE, transferred into Immobilion-PVDF membranes (Merck Millipore, Madrid, Spain) and probed with antibodies against pACC (Ser79) (Cell Signaling; Danvers, MA, USA); and GAPDH (Abcam, Cambridge, UK). Anti-mouse or anti-rabbit horseradish peroxidase-conjugated (Jackson, West Grove, USA) were used as secondary antibodies. LuminataForte Western HRP substrate (Merck Millipore, MA, USA) was used as developing agent. Images were collected by the ChemiDoc MP and Image Lab Software (Bio-Rad Laboratories, Hercules, USA) and quantified by densitometry using ImageJ-1.33 software (NIH, Bethesda, MD, USA). In all the figures showing images of gels, all the bands for each picture come from the same gel, although they may be spliced for clarification.

### 2.12. Immunofluorescence

Mice were anesthetized under ketamine/xylazine and intracardially perfused with PBS and the 10 % Normal Buffered Formalin (NBF). Brains were collected and postfixed 24 h in 10 % NBF at 4 °C, transferred to 30 % sucrose at 4 °C for 2—3 days, frozen in isopentane, and sliced in 30 μm thick slices in the coronal plane throughout the entire rostral-caudal extent of the brain using a cryostat. Slices were preserved at −20 °C in antifreeze solution until use. Sections containing the hypothalamus were processed as previously described [9]. Briefly, sections were blocked in 2 % goat or donkey anti-serum in KPBS and 3 % BSA plus 0.1 % Triton X-100 and incubated with primary antibody (rabbit anti-c-Fos, 1:200, Cell Signaling, Danvers, MA, USA; sheep anti-αMSH, 1:1000, Sigma—Aldrich, Merck KGaA, Darmstadt, Germany) for 1 h at room temperature (RT) or overnight (o/n) at 4 °C, respectively. Goat anti-rabbit Alexa Fluor 647 antibody (1:1000; Invitrogen, Waltham, USA) or donkey anti-sheep Alexa Fluor 488 (1:1000; Invitrogen, Waltham, USA) were used as secondary antibodies. Slices were counterstained with Hoechst for nuclear staining (1 mg/mL, Sigma—Aldrich, Saint Louis, USA). Then, slices were mounted using antifade Fluoromount-G® (0100-01, Southern Biotech, Birmingham, USA) on coverslips (DIO2460, Deltalab, Barcelona, Spain). Images were taken using a Leica DMi8 confocal microscope equipped with a 20× and 40× objective. Fluorescence integrated density after image masking was calculated using ImageJ 1.33 software.

 

### 2.13. Adipose tissue histopathology and adipocyte area measurement

Fixed eWAT were dehydrated and embedded in paraffin. The resulting blocks were cut into 5—10 μm sections and stained with hematoxylin and eosin (H&E) to assess histology. To quantify the adipocyte area, three representative images from each adipose tissue section were taken with a 20× objective using a high-sensitivity camera (Leica MC 190 HD Camera) and microscope. Images were analyzed with the Adiposoft software as described in Zagmutt et al., 2023 [40]. Images were analyzed and adipocytes were highlighted if they met the following criteria: (1) the boundaries for sizing of the cell were 40—40,000; (2) the adipocyte had a shape factor of 0.35—1 (a shape factor of 0 indicated a straight line, while a shape factor of 1 indicated a perfect circle); and (3) the adipocyte did not border the image frame. The results are represented as the average of total area counted.

### 2.14. Oil Red-O liver staining

Livers were collected and fixated 24 h in 10% NBF at 4 °C, transferred to 30% sucrose at 4 °C for 2—3 days, frozen in isopentane, and sliced in 30 μm thick slices using a cryostat. Slices were mounted, fixated with 10% NBF and dehydrated with 90% isopropanol, and then stained with Oil Red-O. Images were obtained with 10× objective using a high-sensitivity camera (Leica MC 190 HD Camera) and quantified using ImageJ-1.33 software.

### 2.15. Analysis of eCBs

Hypothalamic eCBs were analyzed as described in Miralpeix et al., 2019 [42]. Briefly, the hypothalamus (6—8 mg wet tissue) was homogenized with a Dounce tissue grinder with 200 μL of ice-cooled deionized water containing a final concentration of 0.362 μM N-oleylethanolamine-d2 (OEA-d2) (Cayman Chemicals, Ann Arbor, MI) as the internal standard for 2-arachydonoyl (2-AG) and anandamide (AEA) calibration, 100 μM PMSF, and 0.01 % butylated hydroxytoluene (BHT) (Sigma—Aldrich, Madrid, Spain), followed by a brief sonication. After that, lipids were extracted with ethyl acetate/n-hexane (9:1, v/v) and evaporated. eCBs levels were analyzed by LC/MS/MS. 2-AG, AEA, and OEA-d2 were used for the calibration curve in an Acquity ultra-high-performance liquid chromatography (UPLC) (Waters, Singapore) system connected to a Xevo-TQS triple-quadropole Detector (Waters, Ireland) and controlled with Waters/Micromass MassLynx software. Chromatographic separation was performed on an Acquity UPLC BEH C18 column with an isocratic mobile phase of formic acid 0.1 % in water-acetonitrile (30:70, v/v). Detection was performed in the positive ion mode. The capillary voltage was set to 3.1 kV, the source temperature was 150 °C, and the desolvation temperature was 500 °C.

### 2.16. Tissue triglycerides and serum leptin determination

40 mg of tissue (liver or WAT) were homogenized in cold acetone using ceramic beads (32201-1L-M, Sigma—Aldrich, Saint Louis, USA) and Fast-Prep®-24 at 6.5 M/s for 3 cycles of 30 s. Then, samples were incubated in rotatory homogenization o/n at RT. Upper layer was used for TG measurement using Serum Triglyceride Determination kit (TR0100, Sigma Aldrich, Saint Louis, USA). Serum leptin was measured with Mouse Leptin ELISA KIT #90030, Crystal Chem, Grove Village, IL, USA.

### 2.17. Data processing and statistical analysis

Statistical analyses were performed with Prism 9.0 (GraphPad Software, San Diego, USA). Data were expressed as mean ± SEM. Two-way ANOVA test followed by post hoc two-tailed Bonferroni test was applied or a t-student test if only two groups were compared. A p-value less than 0.05 ($p < 0.05$) was considered statistically significant. During data analysis, any outlier data points that deviated from the mean by more than two standard deviations were excluded from the analysis. The mice number and the statistical test used are specified in each figure legend. Animals that showed signs of disease at the time of sacrifice were excluded from the study.

## 3. RESULTS

### 3.1. Generation of SF1-Cpt1c-KO mice

We generated a mouse model with specific deletion of *Cpt1c* in SF1 neurons using the FRT-Flp and Cre-lox recombination technologies as described in the methodology section. We confirmed that SF1-*Cpt1c*-KO mice were properly generated by the amplification of a 531 bp band containing the deletion of exons 4 to 6 of *CPT1c* only when DNA was obtained from VMH but not from hippocampus or cortex brain samples (Figure 1A). Secondly, we observed a pronounced decrease of CPT1C immunodetection in the VMH region (Figure 1B), but not in the ARC (Supplemental Fig. 2). Finally, SF1 neurons were stained by injection of AAV9-EF1a-DIO-mCherry viruses in the VMH (Figure 1C). Figure 1D shows that CPT1C expression in mCherry-positive cells was negligible in SF1-*Cpt1c*-KO mice. The data collectively indicate that the *Cpt1c* gene has been specifically modified in SF1 neurons of the hypothalamus, resulting in the absence of protein expression in these cells.

### 3.2. SF1-Cpt1c-KO mice show normal feeding and energy balance under standard diet

To characterize the phenotype of the mice, we began by monitoring the evolution of food intake, body weight, and adiposity in both male and female mice over a period of 8 weeks while on a standard diet (SD). For adiposity, we measured the amounts of epididymal and subcutaneous white adipose tissue (eWAT and sWAT, respectively), brown adipose tissue (BAT), and total body composition using MRI. Our analysis revealed no significant differences in either parameter between SF1-*Cpt1c*-KO and SF1-*Cpt1c*-WT mice in both sexes (Supplemental Fig. 3A—D and Supplemental Fig. 5A—C). Additionally, we examined various metabolic parameters and found no differences in energy expenditure (EE), respiratory exchange ratio (RER), or locomotor activity between the two genotypes (Supplemental Fig. 3F). We also assessed the function of brown adipose tissue (BAT) by analyzing thermogenesis and found it to be comparable in both male and female mice (Supplemental Fig. 3E and Supplemental Fig. 5D). Moreover, glucose tolerance and insulin sensitivity were comparable between SF1-*Cpt1c*-KO and SF1-*Cpt1c*-WT mice in both sexes (Supplemental Fig. 4 and Supplemental Fig. 5E—K). Notably, male null mice showed an increased rate constant for insulin tolerance test (KITT) compared to their control littermates, although no differences were observed in the area under the curve (AUC) (Supplemental Fig. 4 D-G). Overall, these findings suggest that, under SD conditions, the deficiency of CPT1C in SF1 neurons does not lead to remarkable changes in these physiological or metabolic traits between genotypes in either sex.

### 3.3. SF1-Cpt1c-KO mice exhibit increased food intake, respiratory quotient and adiposity under short-term high-fat challenge

Next, we challenged null mice and their control littermates with HFD. Interestingly, switching the animals to a HFD for just 5 days was enough to reveal significant differences in crucial parameters between genotypes. On the one hand, male SF1-*Cpt1c*-KO mice showed higher food intake, especially during the dark phase (Figure 2A—B), leading to increased body weight and a higher body weight gain (Figure 2C).

 

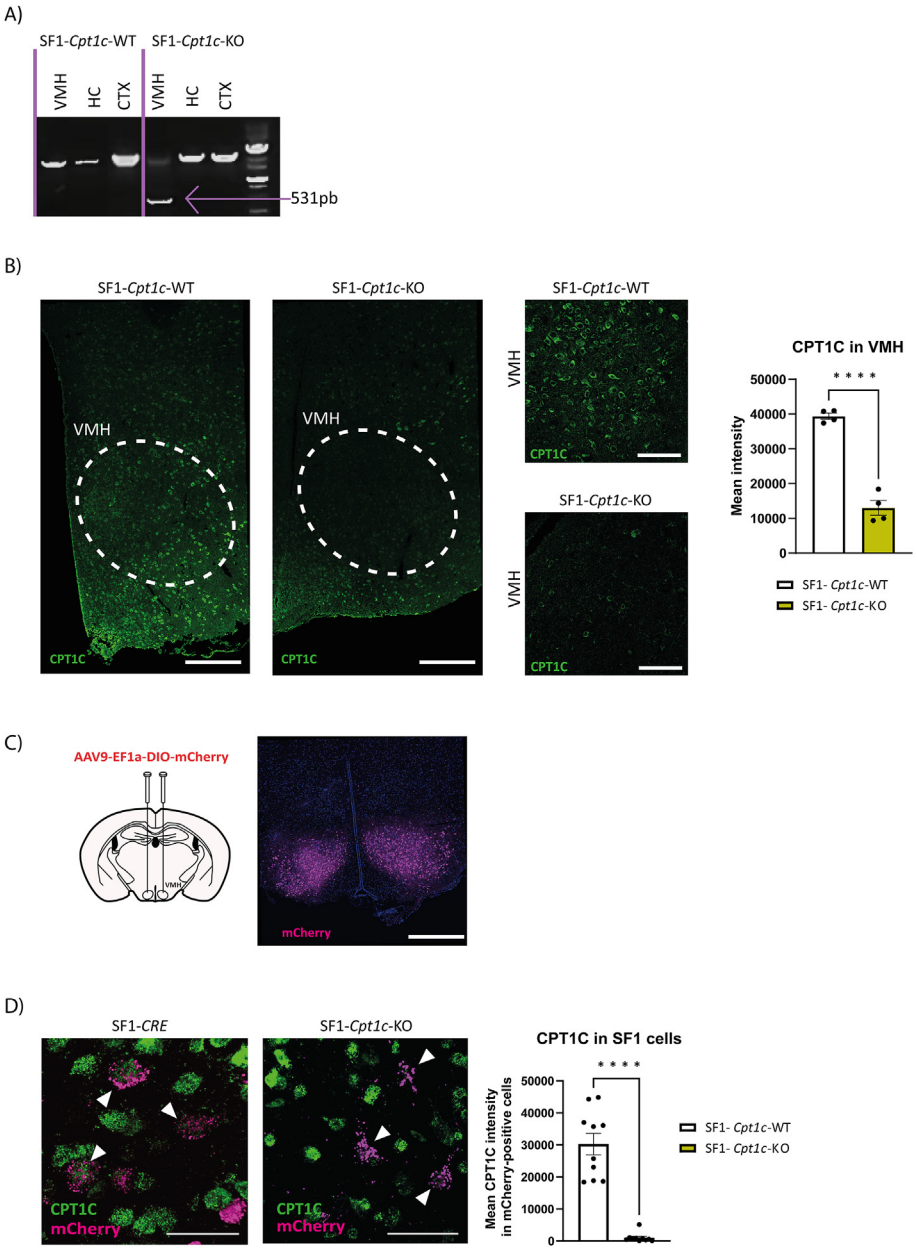


**Figure 1: Validation of SF1-*Cpt1c*-KO mice.** A) PCR amplification demonstrating the excision of exons 4 to 6 of the *Cpt1c* gene in SF1-*Cpt1c*-KO mice. Image of an agarose gel showing PCR products after electrophoresis. Samples were collected from three different brain regions: CTX (cortex), HC (hippocampus), and VMH (ventromedial hypothalamus). A lower-sized band, corresponding to the excision of exons 4–6, is present only in the VMH of SF1-Cpt1c-KO mice. B) Expression of CPT1C in the VMH of SF1-*Cpt1c*-WT and SF1-*Cpt1c*-KO mice. Representative images are shown on the left, and the quantitative analysis is presented on the right. Scale bar: 300 μm. Data are represented as mean ± SEM, male mice, 8–12-week-old, n = 4 per group. ****p < 0.0001 vs SF1-*CPT1c*-WT mice. Statistical significance was determined by the t-student test. C) Left: Schematic representation of the stereotaxic injection of AAV9-EF1a-DIO-mCherry into the VMH. Right: Representative image of VMH region in a brain section from SF1-CRE mice, 3 weeks after AAVs injection. Scale bar: 500 μm. D) Colocalization of CPT1C with mCherry-positive cells 3 weeks after AAV9-EF1a-DIO-mCherry injection in the VMH of SF1-CRE and SF1-*Cpt1c*-KO mice. Representative images of the VMH region in brain sections from both groups are shown on the left, and the quantitative analysis is presented on the right. Both genotypes show CRE activity in SF1 cells of the VMH (mCherry-positive cells); however, in SF1-*Cpt1c*-KO mice, all mCherry-positive cells are CPT1C-negative. Scale bar: 40 μm. Data are represented as mean ± SEM, male mice, 8–12-week-old, n = 10 per group. ****p < 0.0001 vs SF1-*CPT1c*-WT mice. Statistical significance was determined by the t-student test.

Interestingly, SF1-*Cpt1c*-KO mice do not properly accommodate total caloric intake upon dietary change to fats as control animals do (Figure 2D). On the other hand, calorimetric studies showed that the RER of SF1-*Cpt1c*-KO was higher than that of control mice, especially during the dark phase (Figure 2E). This implies that in KO animals subjected to HFD there is a reduced use of fats as the primary fuel source in peripheral tissues compared to control littermates, indicating a failure in metabolic adaptation. MRI analysis revealed an increase of fat mass (Figure 2F) while lean mass remained unchanged (Figure 2G). The increase in fat mass was not due to significant changes in energy

 

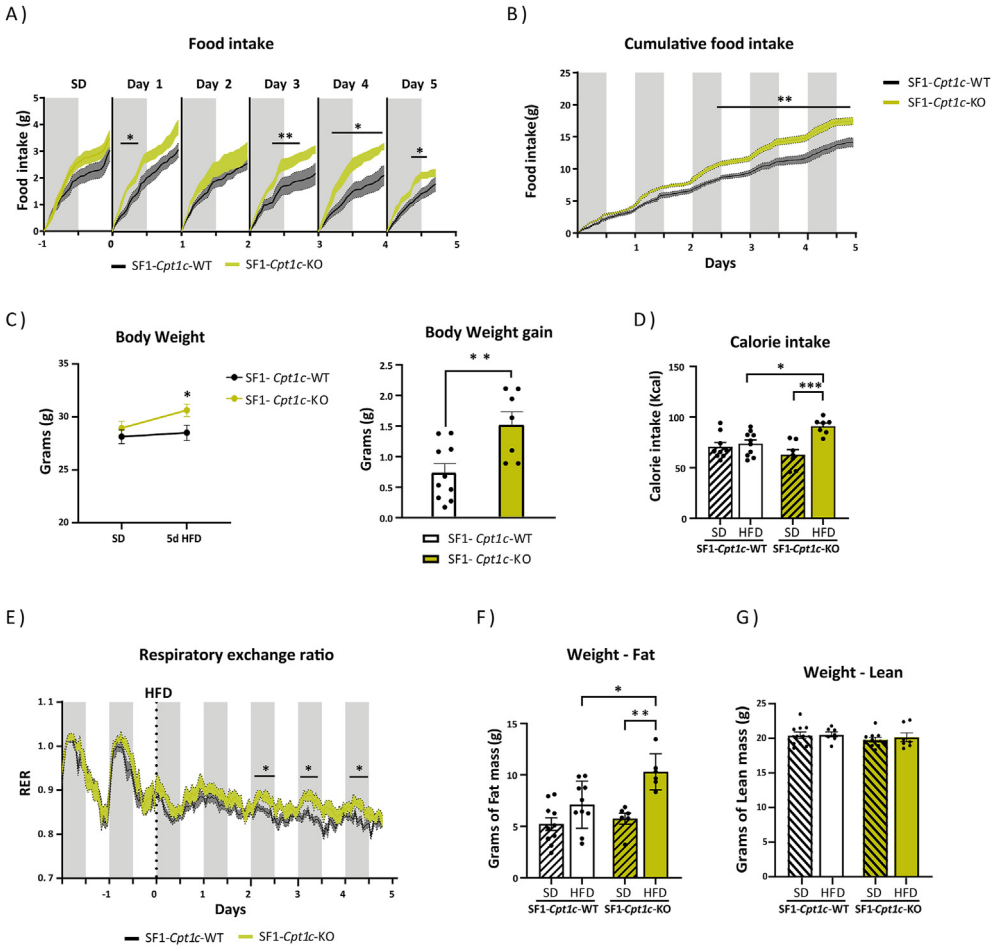


**Figure 2: Metabolic phenotype of male SF1-*Cpt1c*-KO and -WT mice upon 5 days of HFD.** A) Cumulative daily food intake was recorded during both the dark and light phases of each day, starting one day prior to diet change and continuing for 5 days while on the high-fat diet (HFD). B) Cumulative food intake. C) Body weight and body weight gain D) Total calorie intake over the 5 days of HFD. E) Respiratory exchange ratio, starting 2 days prior to diet change and continuing for 5 days while on the HFD. F) Magnetic Resonance Imaging (MRI) analysis of fat mass of mice in SD and 5 days of HFD. G) Magnetic Resonance Imaging (MRI) analysis of lean mass of mice in SD and 5 days of HFD. Data are represented as mean ± SEM, male mice, 8–12-week-old, n = 7–10/group. *p < 0.05, **p < 0.01, ***p < 0.001 vs SF1-*CPT1c*-WT mice. Statistical significance was determined by ANOVA test with post-hoc Bonferroni.

expenditure, BAT thermogenesis or locomotor activity (Supplemental Fig. 6A–C). Moreover, leptin levels remained similar between genotypes (Supplemental Fig. 6D). Collectively, these data suggest that CPT1C deficiency in SF1 neurons impairs early metabolic adjustment to increased consumption of fats.

The experiment was repeated ensuring that both groups of animals consumed the same amount of food (pair-feeding). As shown in Figure 3, while the animals' food intake was identical between genotypes (Figure 3A), the SF1-*Cpt1c*-KO mice showed a tendency to gain more weight and fat (Figure 3B–E), along with a higher accumulation of lipids in the liver (Figure 3F). These results suggest that the increased adiposity and weight observed in SF1-*Cpt1c*-KO animals is not only due to increased food intake but also to a dysfunction in lipid allocation.

### 3.4. Impaired lipid metabolism in SF1-Cpt1c-KO mice following short-term HFD

Next, we analyzed lipid metabolic enzymes in peripheral tissues, such as the liver, sWAT eWAT, and muscle, in animals fed a HFD for 5 days. qPCR studies showed that mRNA expression of liver lipolytic enzymes, such as adipose triglyceride lipase (ATGL) and hormone-sensitive lipase (HSL), and the rate-limiting enzyme of fatty acid oxidation, CPT1A, were decreased while the lipogenic stearoyl-CoA desaturase 1 (SCD1) was increased (Figure 4A). In relation to lipoprotein lipase (LPL) and CD36, two markers associated with lipid uptake and tissue triglycerides (TG) accumulation [43] their expression increased during the diet switch (after 5 days of HFD) in SF1-*Cpt1c*-KO mice but not in control littermates (Figure 4B–C). Conversely, fatty acid synthase (FASN) expression decreased in both genotypes (Figure 4D). These collective data suggest an enhanced storage of lipids in liver of male SF1-C*pt1c*-KO mice, attributed to increased fatty acid uptake combined with reduced rates of lipolysis and fatty acid oxidation. Accordingly, liver TG and Oil Red-stained fat depots were higher in SF1-*Cpt1c*-KO mice than in control mice after only 5 days of HFD (Figure 5A–B).

Similar results were observed in the eWAT of SF1-*Cpt1c*-KO mice. ATGL was decreased while lipogenic markers such as ACCa and FAS were increased (Figure 4E), resulting in TG accumulation and larger adipocyte size (Figure 5C–D). In sWAT, ATGL levels remained unchanged, but the expression levels of two adipokines secreted during adipogenesis and associated with obesity, namely leptin and FABP4, were higher in SF1-*Cpt1c*-KO mice than in SF1-*Cpt1c*-WT animals

 

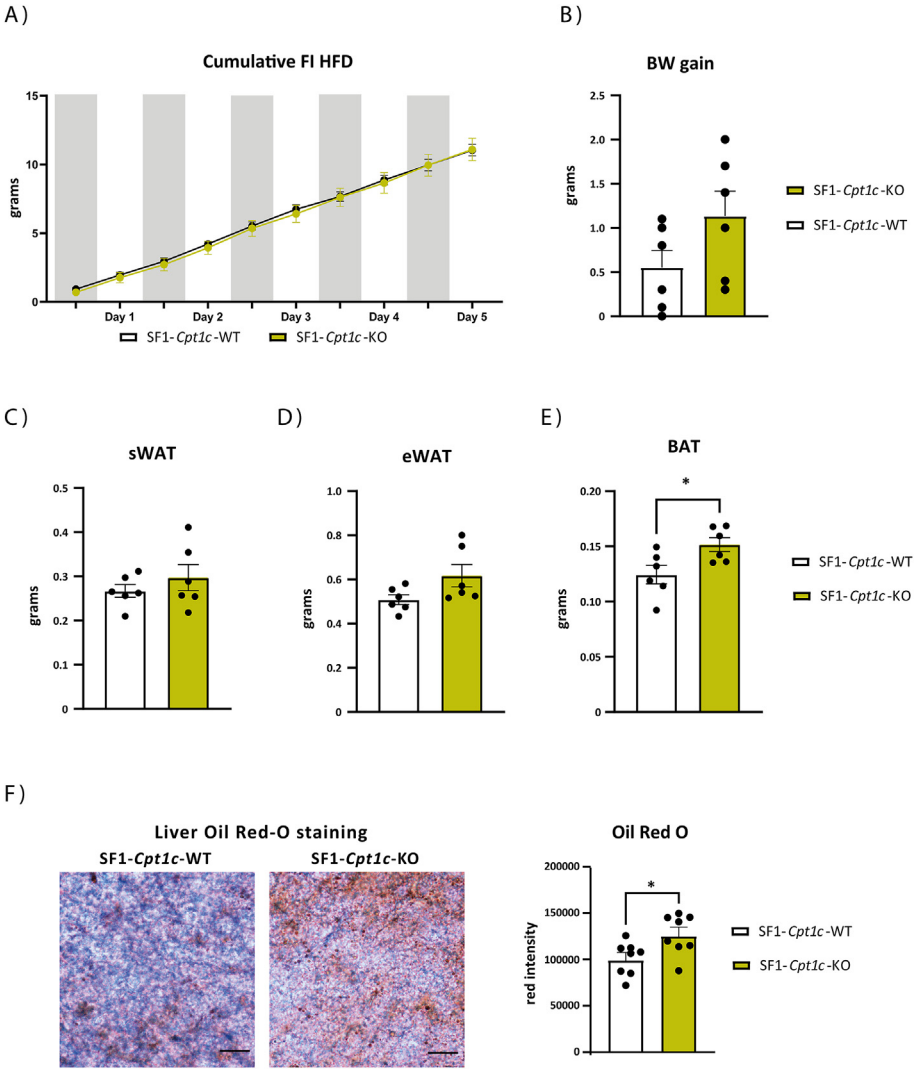


**Figure 3: Metabolic phenotype of male SF1-*Cpt1c*-KO and -WT mice upon 5 days of pair feeding with a HFD.** A) Cumulative food intake. B) Body weight gain. C) Subcutaneous White Adipose Tissue (sWAT) weight. D) Epididymal White Adipose Tissue (eWAT) weight. E) Brown Adipose Tissue (BAT) weight. F) Oil Red-O staining of liver sections from SF1-*Cpt1c*-KO and -WT mice fed a SD or a HFD for 5 days, and quantification. Scale bar: 100 μm. Data are represented as mean ± SEM, male mice, 8–12-week-old, n = 7–10/group. *p < 0.05, **p < 0.01, ***p < 0.001 vs SF1-*Cpt1c*-WT mice. Statistical significance was determined by ANOVA test with post-hoc Bonferroni. (For interpretation of the references to color in this figure legend, the reader is referred to the Web version of this article).

(Figure 4F). No variations were found in the expression of β-3 adrenergic receptor (β3AR) in either eWAT or sWAT, in accordance with no changes in EE.

Differences between genotypes were also evident in the soleus muscle. SF1-*Cpt1c*-KO mice exhibited lower expression levels of PPARδ and CPT1B (Figure 4G), along with reduced phosphorylation levels of ACC, which is indicative of decreased FAO in muscle (Figure 4H) (Liu et al., 2018).

Finally, serum TG and total cholesterol levels were analyzed (Supplemental Fig. 6E–F). Results show a reduction in serum TG levels in SF1-*Cpt1c*-KO mice compared to controls, while no significant differences were observed in cholesterol levels. Since TG levels were significantly higher in the liver and adipose tissue of KO mice, these findings suggest increased TG uptake and storage, associated with higher LPL expression in peripheral tissues (enhancing TG clearance from the blood), as well as reduced TG release into circulation by the liver.

### 3.5. SF1-Cpt1c-KO mice develop obesity and exhibit insulin resistance during long term HFD exposure

Maintaining animals on a HFD for a longer period (8 weeks) resulted in greater differences between genotypes in adiposity and body weight in both sexes (Figure 6A–F and Supplemental Fig. 7A–D). Interestingly, male SF1-*Cpt1c*-KO mice exhibited a more pronounced obesogenic phenotype compared to females, as weight gain differences relative to control littermates became apparent earlier in males. Furthermore, the increase in fat mass (eWAT and BAT) was more pronounced in males than in females. On the other hand, increased adipocyte size (Figure 6G), and alterations in the expression of some lipid metabolic markers in peripheral tissues (Figure 6H) were observed in SF1-*Cpt1c*-KO mice compared to control littermates. Notably, these effects were feeding-independent, as the amount of food consumed was the same in both genotypes (Figure 6B and Supplemental Fig. 7C). However, when analyzing food intake over 5-day periods, we observed an increase in consumption occurring only during the first 5 days following

 

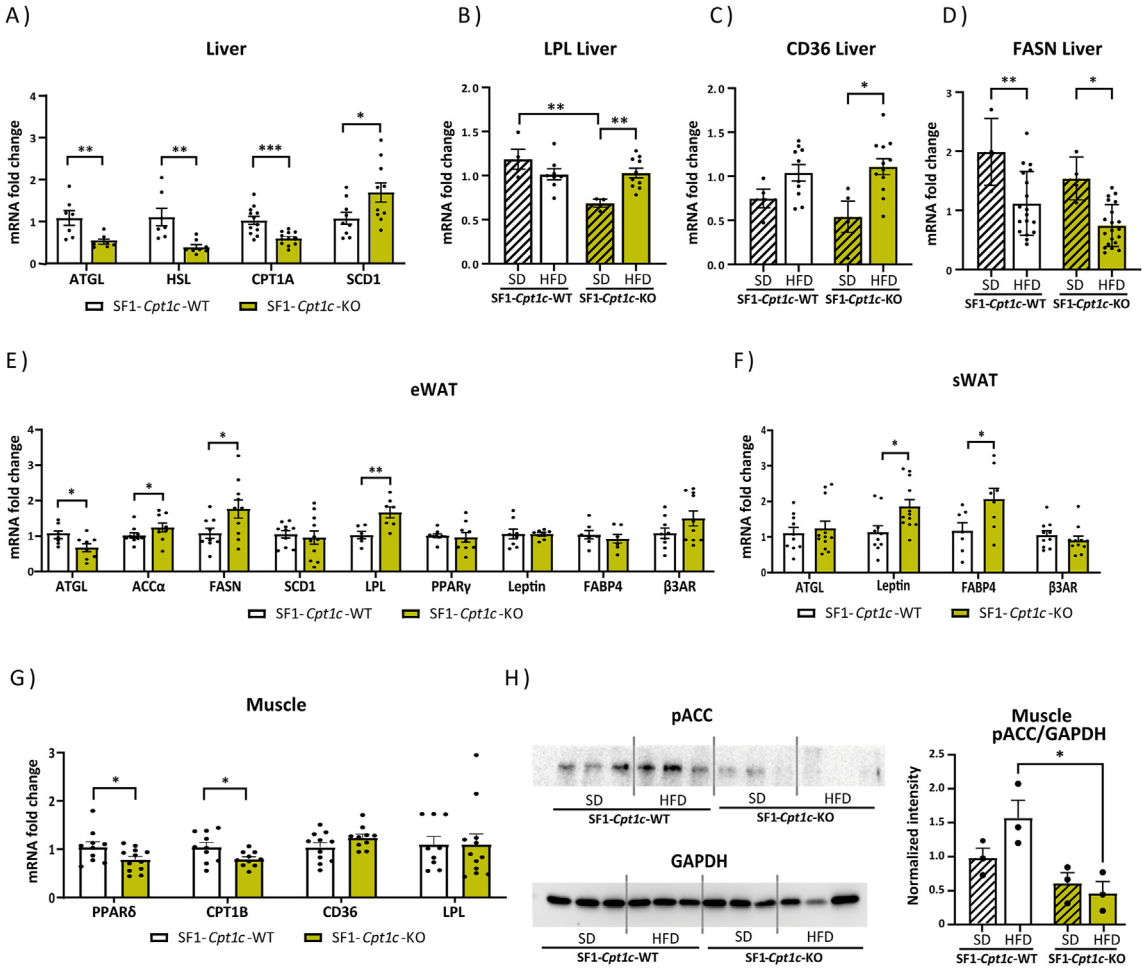


**Figure 4: Expression of proteins and hormones involved in lipid metabolism in different tissues of male SF1-*Cpt1c*-KO and -WT mice after 5 days of HFD.** A) Expression of adipose triglyceride lipase (ATGL), hormone-sensitive lipase (HSL), CPT1A, stearoyl-CoA desaturase (SCD1) measured by qPCR in liver samples of mice fed a HFD for 5 days. B) Lipoprotein lipase (LPL) expression in liver samples. C) CD36 expression in liver samples. D) Fatty acid synthase (FAS) expression in liver samples. E) Expression of ATGL, acetyl-CoA carboxylase-alpha (ACCα), FAS, SCD1, LPL, peroxisome proliferator-activated receptor gamma (PPARγ), leptin, fatty acid-binding protein 4 (FABP4) and beta-3 adrenergic receptor (β3AR) in epididymal WAT (eWAT). F) ATGL, leptin, fatty acid-binding protein 4 (FABP4) and β3AR expression in subcutaneous WAT (sWAT). G) PPARδ, CPT1B, CDC36 and LPL expression in gastrocnemius muscle. H) Western blot (a representative image) of pACC and GAPDH from muscle samples and the quantification of pACC normalized by GAPDH. Data are represented as mean ± SEM, male mice, 8–12-week-old, n = 3–12/group, $^{*}p < 0.05$, $^{**}p < 0.01$, $^{***}p < 0.001$. Statistical significance was determined by ANOVA test with post-hoc Bonferroni.

the diet change, with differences dissipating in subsequent days (Supplemental Fig. 8A). This indicates that SF1-Cpt1c-KO mice exhibit transient hyperphagia and adjust their intake to increased dietary fat at a delayed rate compared to control mice.

After 8 weeks of HFD feeding, SF1-Cpt1c-KO male mice exhibited higher plasma leptin levels (Figure 7A) and showed greater glucose intolerance and insulin resistance compared to their control littermates (Figure 7B–C). In females, the alterations in glucose homeostasis were less pronounced, as only glucose intolerance was observed, without evidence of insulin resistance (Supplemental Fig. 7E–F). This is consistent with the delayed development of obesity observed in female mice. Taken together, the data suggest that CPT1C KO mice are unable to adequately adapt their peripheral metabolism to HFD, making them more prone to developing obesity and glucose intolerance in the long term.

### 3.6. The melanocortin signaling is hindered in SF1-Cpt1c-KO mice

Next, we investigated the underlying molecular mechanisms occurring in the hypothalamus of SF1-Cpt1c-KO mice. We focused on the early period following the dietary change—5 days of HFD—as the animals already showed significant weight gain and adiposity during this phase.

We first analyzed the hypothalamic expression of orexigenic and anorexigenic peptides due to the hyperphagic response observed in SF1-CPT1c-KO mice after switching from SD to HFD. The mRNA expression of the satiating neuropeptide precursor POMC was decreased, while the orexigenic neuropeptide AgRP was increased in SF1-Cpt1c-KO mice compared to control mice, which could explain the increased food intake (Figure 8A). In contrast, NPY expression was decreased. Given that POMC and AgRP directly influence the melanocortin system, α-MSH levels were measured. Consistently, α-MSH staining was significantly reduced in the ARC and mildly diminished in the PVN of SF1-*Cpt1c*-KO mice upon short-HFD compared to control mice (Figure 8B–D), suggesting an impaired activation of the melanocortin system following dietary change. This impairment could be responsible for the hyperphagia and adiposity observed in KO mice [44,45].

 

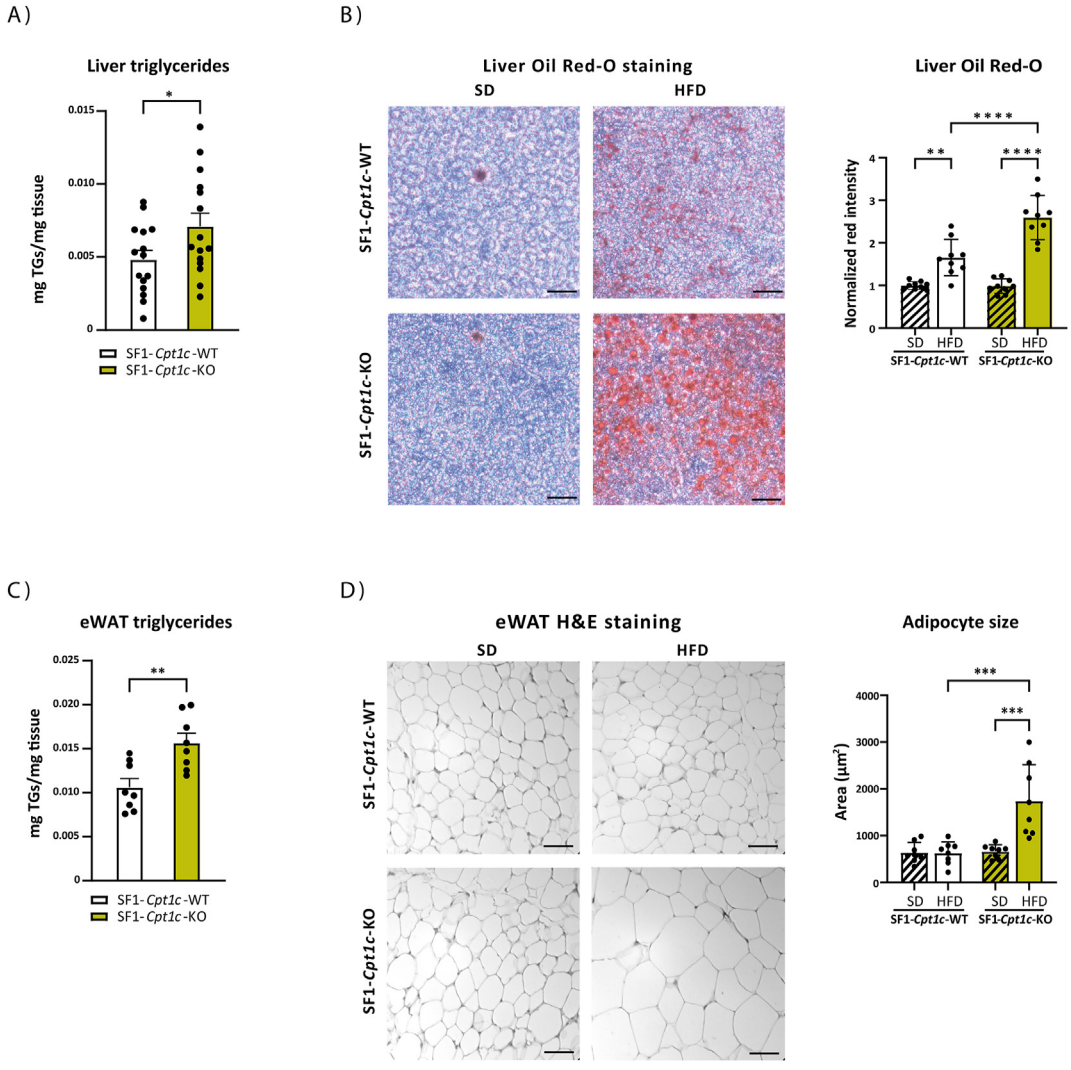


**Figure 5: Liver and eWAT adiposity of male SF1-*Cpt1c*-KO and -WT mice after 5 days of HFD.** A) Liver triglycerides (TG) after 5 days of HFD B) Oil Red-O staining of liver sections from SF1-*Cpt1c*-KO and -WT mice fed a SD or a HFD for 5 days, and quantification. Scale bar: 100 µm. C) eWAT triglycerides. D) Hematoxylin and eosin staining of eWAT sections and quantification of adipocyte size. Scale bar: 50 µm. Data are represented as mean ± SEM, male mice, 8–12-week-old, n = 8–9/group, *p < 0.05, **p < 0.01, ***p < 0.001. Statistical significance was determined by ANOVA test with post-hoc Bonferroni. (For interpretation of the references to color in this figure legend, the reader is referred to the Web version of this article).

### 3.7. The eCB system is altered in the hypothalamus of SF1-*Cpt1c*-KO mice

Then, we analyzed the endocannabinoid system, since we previously reported that short-term exposure to a HFD increases eCBs levels in the hypothalamus [42]. Moreover, CB1 receptor is highly expressed in SF1 neurons [10], regulates the SF1-POMC drive, and it is involved in the regulation of peripheral lipid metabolism [11].

The analysis of hypothalamic eCB levels revealed that SF1-Cpt1c-KO mice upon SD show higher levels of both eCBs, anandamide (AEA) and 2-arachidonoylglycerol (2-AG), in the hypothalamus compared to control mice (Figure 9A), indicating a basal impairment of the eCB system. After five days of HFD, control animals increased hypothalamic 2-AG, as previously described [42], but no further changes were observed in SF1-*Cpt1c*-KO. Regarding AEA, although both genotypes exhibit reduced levels after five days of HFD compared to SD, those detected in KO mice consistently remained elevated compared to control mice. Importantly, there were no significant differences in endocannabinoid levels between the various diets or genotypes in the hippocampus (Supplemental Fig. 9A and B). This indicates that the changes observed are specific to the hypothalamus.

We then measured the expression of eCBs synthesis and metabolizing enzymes in the hypothalamus. qPCR results showed that the expression of monoglyceride lipase (MGLL) and fatty-acid amide hydrolase 1 (FAAH), the main metabolizing enzymes of 2-AG and AEA, respectively, were decreased in SF1-*Cpt1c*-KO mice fed a HFD (Figure 9B), suggesting that these metabolic enzymes could play a role in eCB accumulation. No changes were observed in the expression of ABHD6, another hydrolase that contributes to a lesser extent to the metabolism of 2-AG (Supplemental Fig. 9C). Regarding the major neuronal enzyme involved in 2-AG synthesis, diacylglycerol lipase-alpha (DAGLα), no changes were observed, whereas the one involved in AEA synthesis, N-acyl-phosphatidylethanolamine-hydrolyzing phospholipase D (NAPE-PLD), exhibited a decrease, probably due to a compensatory response.

We also analyzed CB1 receptor expression and found that short-term HFD increases CB1 expression in control mice (Figure 9C), indicating

 

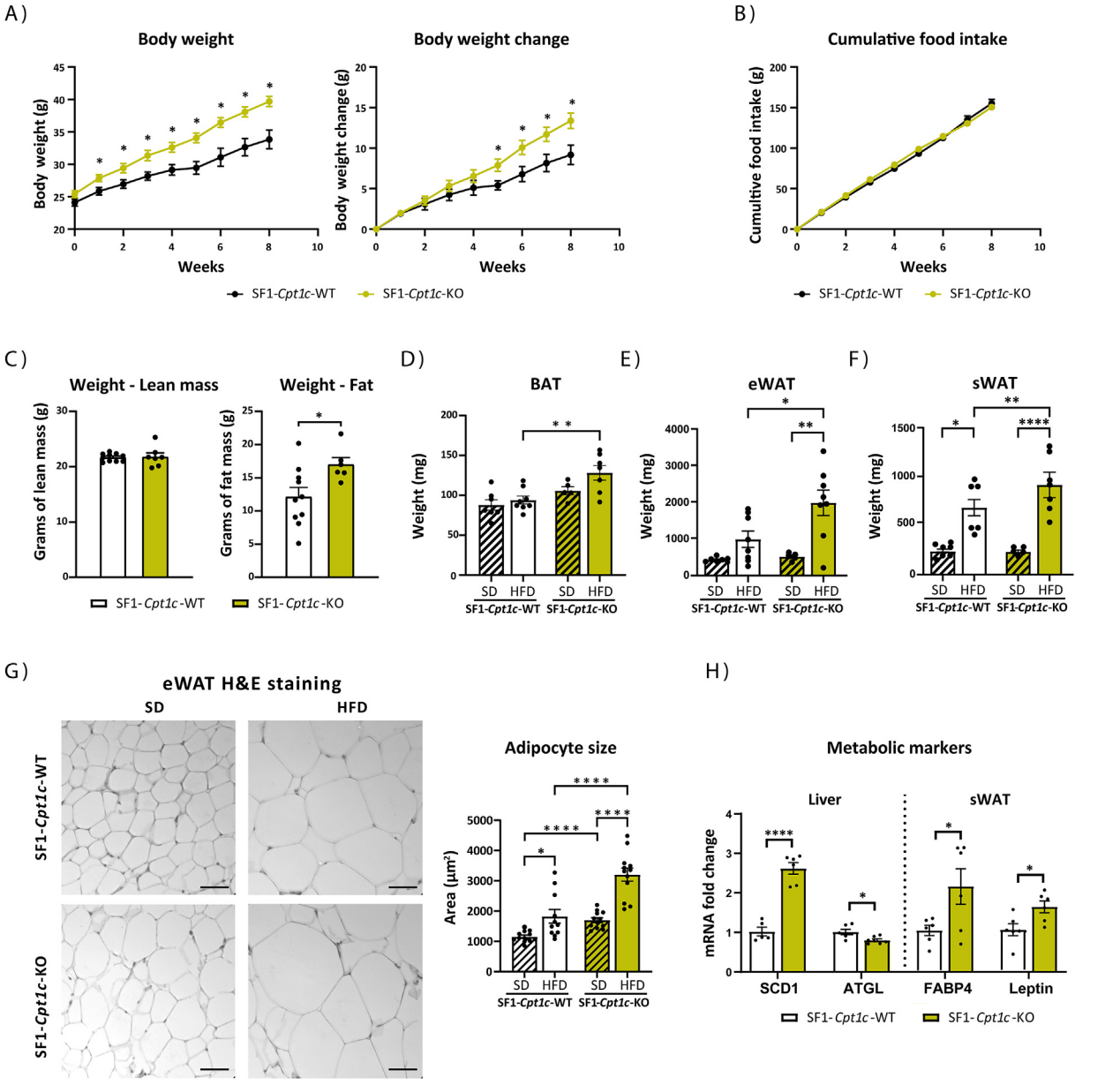


**Figure 6: Metabolic phenotype of male SF1-*Cpt1c*-KO and -WT mice after 8 weeks of HFD.** A) Body weight and body weight gain. B) Cumulative food intake measured once per week. C) MRI analysis of lean and fat mass. D) BAT weight. E) eWAT weight. F) sWAT weight. G) Hematoxylin and eosin staining of eWAT sections (representative images) and the quantification of adipocyte size. Scale bar: 50 µm. H) Expression of SCD1 and ATGL in liver samples, and FABP4 and leptin in sWAT samples of SF1-*Cpt1c*-KO and -WT mice after 8 weeks of HFD. Data are represented as mean ± SEM, male mice, 16-week-old, n = 8–10/group (for H&E staining 2 slices/mouse). *p < 0.05 **p < 0.01, ***p < 0.001, ****p < 0.0001. Statistical significance was determined by ANOVA test with post-hoc Bonferroni.

an activation of the eCB system following dietary change. However, this increase was not observed in SF1-*Cpt1c*-KO mice. Taken together, SF1-*Cpt1c*-KO animals have elevated baseline levels of eCBs under SD conditions and exhibit an anomalous response in their dynamics when switched to a HFD.

### 3.8. Fatty acid sensing in VMH is disrupted in SF1-Cpt1c-KO mice

Since fatty acids are known to signal satiety and lipid metabolism changes through their action on the hypothalamus [9], we decided to determine whether SF1-*Cpt1c*-KO had a defect in FA sensing at the VMH. We injected oleic acid ICV in male mice fed a SD and measured cFOS activation after 2 h. In control mice, oleic acid injection triggered the activation of the VMH (Figure 9D); however, this was not observed in SF1-*Cpt1c*-KO animals. Those findings indicate that CPT1C in SF1 neurons is necessary for proper sensing of fats in the VMH. Probably, the increase in the eCB tone is contributing to this lack of activation [10].

In summary, the absence of CPT1C specifically in SF1 neurons leads to heightened levels of hypothalamic endocannabinoids and compromised sensing of FA in the VMH. This, in turn, disrupts short-term accommodation of food intake, and impairs peripheral lipid metabolism, leading to an obesogenic phenotype over the long term.

 

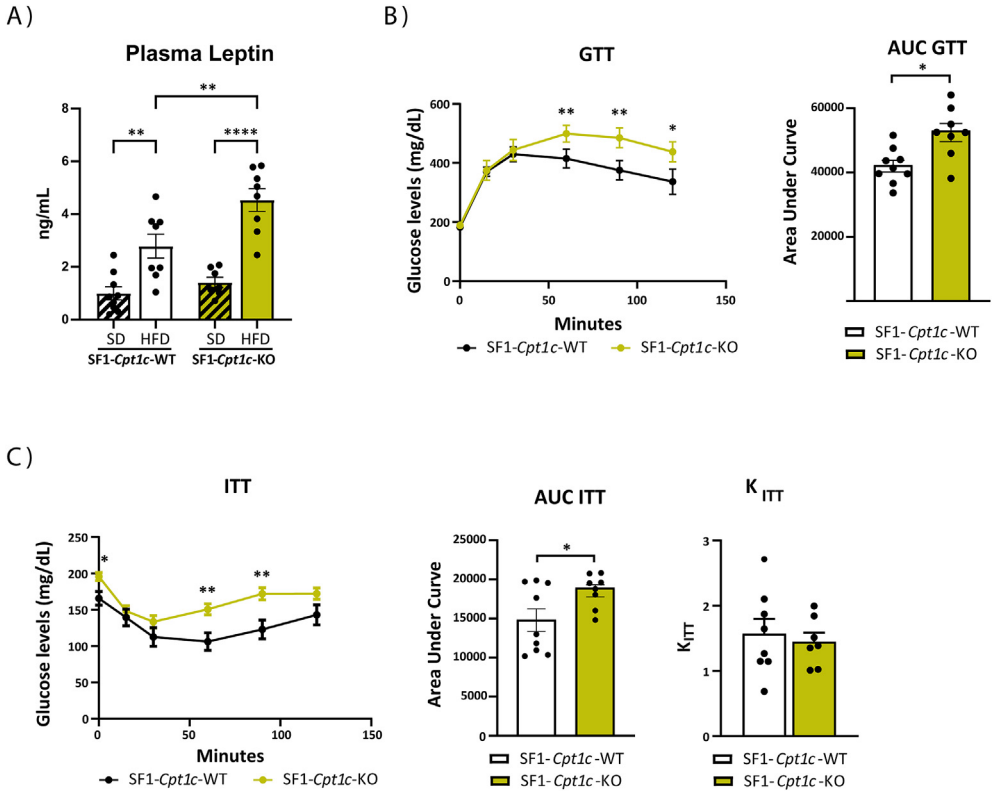


**Figure 7: Plasma leptin levels and glucose homeostasis parameters of male SF1-Cpt1c-KO and -WT mice after 8 weeks of HFD.** A) Plasma leptin levels. B) Glucose tolerance test (GTT) and quantification of the area under the curve (AUC). C) Insulin tolerance test (ITT) and quantification of the AUC and the KITT calculated on the first 30 min of ITT. Data were represented as mean ± SEM, n = 8–10/group. *p < 0.05, **p < 0.01, ****p < 0.0001. Statistical significance was determined by ANOVA test with post-hoc Bonferroni (GTT and ITT curves) and by t-student test (AUC and KITT).

## 4. DISCUSSION

CPT1C is a neuron-specific nutrient sensor [21,24]. It is well known that CPT1C participates in the hypothalamic control of food intake and energy metabolism [13–15,18,25,46]; however, its function in specific neuronal populations has not been explored until now. This study underscores the important role of CPT1C in SF1 neurons of the VMH in sensing fats and favoring early metabolic adaptations to a dietary change.

It has been reported that when switching from a high-carbohydrate diet to a HFD, there is a transient hyperphagia in the initial days, followed by an adjustment in food intake over the following days to maintain total caloric intake [47,48]. Moreover, a metabolic shift occurs in tissues such as the liver, muscle, and adipose tissue, favoring fat as the primary energy source and leading to a decrease in the RER. This shift promotes fat mobilization and short-term maintenance of body weight. Our results show that the absence of CPT1C in SF1 neurons disrupts these processes, delaying the adjustment of food intake and impairing metabolic adaptation in peripheral tissues, leading to increased adiposity and a more rapid development of obesity when maintained on a HFD.

Regarding food intake, the data show that SF1-*Cpt1c*-KO mice show transitory hyperphagia upon exposure to a diet rich in fats, compared to control mice. The impaired expression of orexigenic and anorexigenic neuropeptides and the reduced presence of α-MSH in the ARC are indicative of the inadequate satiety signaling and impaired activation of the melanocortin system in the short-term. It is well known that SF1 neurons provide a robust source of glutamatergic excitatory input onto POMC neurons of the ARC to drive satiety, and that this drive is sensitive to nutrients [49–52]. Our data show that 5 days of HFD consumption in control mice enhances melanocortin signaling to inhibit excessive calorie consumption. However, this effect is attenuated in SF1-*Cpt1c*-KO mice, which is consistent with the hyperphagia observed in these animals. Recently, it has been demonstrated that SF1 neurons also contribute to the satiety signal through innervation of the paraventricular thalamus (PVT) [6]. Therefore, other downstream circuits of SF1 neurons, beyond the melanocortin system, may also contribute to the hyperphagia observed in KO mice.

Regarding nutrient partitioning, SF1-*CPT1c*-KO mice exhibit a decreased preference for fats as a fuel substrate in the liver and muscle, evidenced by diminished lipolysis and cellular FAO in those tissues. Additionally, in WAT, the enzymes involved in lipid synthesis and storage are increased compared to WT animals. Consequently, there is an increase in adiposity and body weight, and, in the long term, leptin resistance and impaired glucose homeostasis. The pair-feeding study indicates that the increase in adiposity in KO mice is independent of food intake. Previous studies have shown that blocking the melanocortin system leads to a decrease in muscle lipolysis and favors WAT expansion in a way that is independent of food intake [44,45]. In these studies, the metabolic alterations are accompanied by an increase in RER, while EE remains unchanged. Considering that the metabolic changes observed in SF1-*Cpt1c*-KO mice align closely with those observations, we suggest that the lack of activation of the melanocortin system in response to fats can also contribute to the metabolic alterations observed in KO mice. Other mechanisms can be involved as SF1 neurons, through nuclei in the brainstem or the preoptic area, are also capable of influencing peripheral tissue metabolism [53,54].

  

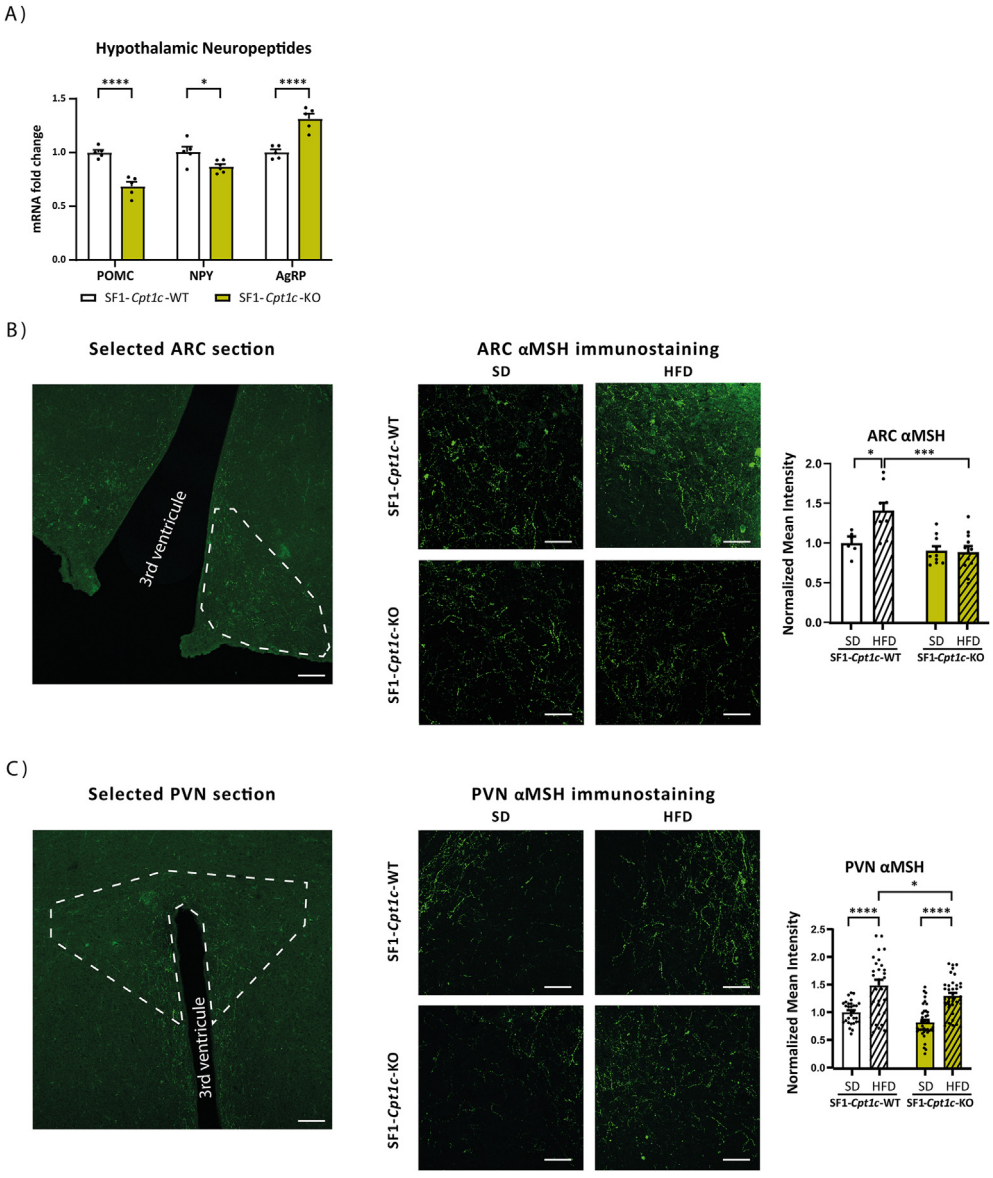


**Figure 8: Hypothalamic neuropeptides and alpha-melanocyte stimulating hormone αMSH).** A) Hypothalamic expression of POMC, NPY and AgRP neuropeptides in male SF1-*Cpt1c*-KO and -WT mice after 5 days on a HFD. B) Left: Representative image of the arcuate nucleus (ARC) indicating the selected area for measuring αMSH levels. Middle: Representative image of αMSH staining in the ARC. Right: Data quantification. C) Left: Representative image of the paraventricular nucleus (PVN) indicating the selected area for measuring αMSH levels. Middle: Representative image of αMSH staining in the PVN. Right: Data quantification. Data are represented as mean ± SEM, male mice, 8–12-week-old, n = 4–7/group (2–5 slices/mouse). *p < 0.05, ***p < 0.001, ****p < 0.0001 vs SF1-*CPT1c*-WT. Statistical significance was determined by two-way ANOVA test with post-hoc Bonferroni. Scale bar: 85 μm.

Notably, selective CPT1C deficiency in SF1 neurons does not appear to play a role in thermogenesis activation in response to a HFD, since no differences were observed in thermogenic markers between genotypes after leptin injection or short-high fat feeding. However, the whole-body CPT1C KO mice did show impaired thermogenesis [16], suggesting that these effects must be mediated by CPT1C in neurons other than SF1 neurons.

Regarding the molecular mechanisms that are responsible for the failure in the proper activation of SF1 neurons upon diet change, we propose the endocannabinoid system as the primary factor. SF1-*Cpt1c*-KO mice exhibit notably elevated levels of the two main eCBs, 2-AG and AEA, in hypothalamus under normal conditions, when fed a SD. eCB are retrograde neuromodulators that fine-tune the hypothalamic circuits favoring food intake and energy accumulation [55]. An elevated tone of the eCB system in the hypothalamus has been associated with an obesogenic phenotype [11,56,57]. Consequently, the permanent increase of eCB levels observed in hypothalamus of SF1-*Cpt1c*-KO mice could potentially explain the predisposition to weight gain observed in those animals. Additionally, the dynamic of 2-AG in response to the short-term HFD is altered and unlike control mice, there is no observed increase in 2-AG, since 2AG is already elevated in SD. Interestingly, the transient elevation of hypothalamic eCBs in response to a HFD has been associated with a protective role against obesity [42]. However, a sustained elevation of these eCBs correlates with a clearly obesogenic phenotype [55].

 

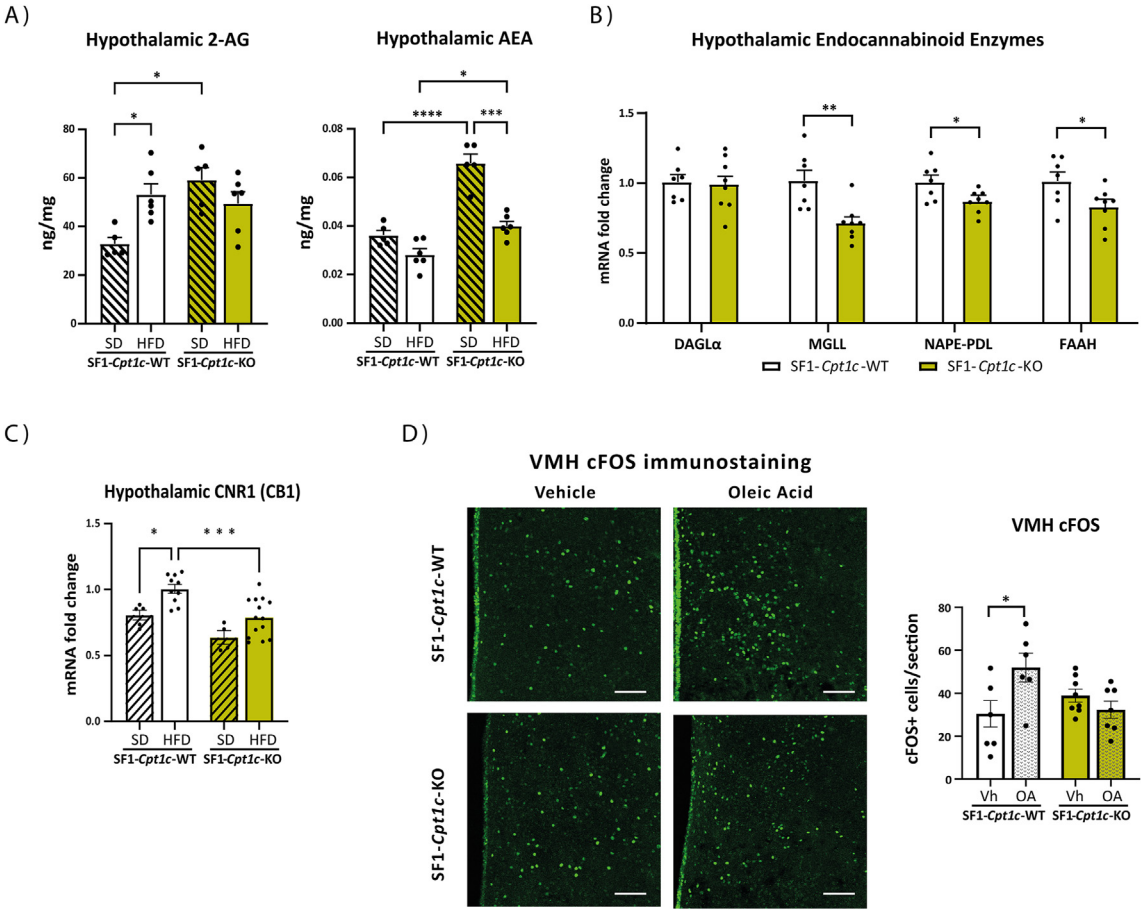


**Figure 9: Endocannabinoid (eCB) system and oleic acid sensing in the hypothalamus of male SF1-*Cpt1c*-KO and -WT mice.** A) Hypothalamic levels of 2-arachidonoylglycerol (2-AG) and anandamide (AEA). B) Hypothalamic expression of enzymes involved in the eCB system: diacylglycerol lipase alpha (DAGLα), monocylglycerol lipase (MGLL), N-acylphosphatidylethanolamine phospholipase D (NAPE-PLD) and fatty acid amide hydrolase 1 (FAAH). C) Hypothalamic expression of the eCB receptor CB1. D) Effects of intracerebroventricular oleic acid (OA) administration on neuronal activation, assessed by cFOS expression in the VMH. Representative images and quantification of c-Fos positive cells per section. n = 3/group (2–3 slices/mouse). bar: 100 μm. Data from A–C panels are represented as mean ± SEM, 8–12-week-old, n = 8–10/group. *p < 0.05 **p < 0.01, ***p < 0.001, ****p < 0.0001, compared to SF1-*Cpt1c*-WT or to the same genotype on SD. Statistical significance was determined by ANOVA test with post-hoc Bonferroni.

Studies have shown that the primary neuronal endocannabinoid receptor, CB1, is predominantly expressed in SF1 neurons compared to other neuronal populations in the mediobasal hypothalamus [10]. Activation of CB1 receptors by agonists decreases the frequency of action potentials and firing rate of SF1 neurons [10]. In our study, increased basal levels of eCBs in the hypothalamus may explain why intracerebroventricular injection of oleic acid fails to activate VMH neurons in SF1-*Cpt1c*-KO mice, whereas it does in control mice. These data confirm the role of CPT1C in nutrient sensing, specifically in fatty acid detection by SF1 neurons.

It has been described that eCBs decrease the excitatory glutamatergic input from SF1 neurons onto POMC [49]. The increase in eCB tone in KO mice could explain the attenuation of the melanocortin system observed in SF1-*Cpt1c*-KO mice in response to a HFD. Additionally, it is known that down-regulation of the SF1-POMC circuitry by the eCB tone is more pronounced in males than in females due to testosterone and the lack of estrogens, making them more sensitive and prone to obesity [49,50]. In our model, we also observe this sexual dimorphism, as male KO mice gained more weight than females and, in the long term, developed obesity more rapidly and showed a more pronounced impairment in glucose homeostasis.

The mechanism by which CPT1C deficiency increases eCB levels remains unknown. Enzyme expression data suggest that this may be due to reduced degradation of these neuromodulators, as the expression of MGLL and FAAH hydrolases are decreased in the hypothalamus of KO mice compared to WT mice. Additionally, the activity of the ABHD6 hydrolase may be altered, although no changes in its expression were observed. We recently reported that CPT1C interacts with and regulates ABHD6 activity in a nutrient-dependent manner [26]. Furthermore, ABHD6 deficiency specifically in the VMH leads to metabolic inflexibility, preventing animals from adapting to metabolic challenges such as high-fat feeding [58]. Further research is required to fully understand how CPT1C affects eCB levels.

In addition to the eCBs, other CPT1C-down-stream mechanisms might be involved. It is well known that CPT1C regulates the abundance of glutamate AMPA receptors in synapsis, synaptic function and spinogenesis in response to nutrients [22,38,59,60]. We could hypothesize that impaired synaptic plasticity of SF1 neurons in SF1-*Cpt1c*-KO mice could contribute to the metabolic inflexibility observed in response to dietary fats.

In summary, our results demonstrate that CPT1C deficiency in SF1 neurons elevates basal eCB levels in the hypothalamus and

 

impairs the sensing of dietary fats. Consequently, animals fail to properly adjust total caloric intake and fuel selection when transitioning from a SD to a HFD, resulting in impaired fat allocation and the development of obesity, along with long-term disruption of glucose homeostasis. These findings provide new insights into the essential role of SF1 neurons in fat sensing and early metabolic adaptation necessary for short-term body weight maintenance. Furthermore, they may contribute to a better understanding of obesity development.

## ACKNOWLEDGEMENTS

This study was supported by the Spanish Ministry of Science and Innovation (PID2020-114953RB-C22 and PID2023-146716OB-I00 to NC and RRR, PID2020-114953RB-C21 to LH and DS, PID2021-128145NB-I00 to ML) co-funded by the European Regional Development Fund, the Centro de Investigación Biomédica en Red-Fisiopatología de la Obesidad y Nutrición (CIBEROBN) (Grant CB06/03/0001 to LH), the Merck Health Foundation (to LH), the Government of Catalonia (2021SGR00367 to LH) and Xunta de Galicia (predoctoral fellowship to to OF-A; ED481A-2019/026). The authors would also like to acknowledge the INSERM (D.C. and P.Z.), Nouvelle-Aquitaine Region (D.C.) Agence Nationale de la Recherche (ANR-18-CE14-0029, ANR-21-CE14-0018, ANR-22-CE14-0016, ANR-23-CE14-0037, ANR-10-LABX-43 and ANR-10-EQX-008-1 to D.C.), the University of Bordeaux's IdEx 'Investments for the Future' program/GPR BRAIN_2030 (D.C.) and the Fondation pour la Recherche Médicale (EQU202303016291 to D.C.; FRM-SPF202004011774 to C.M.). The graphical abstract was created using BioRender (https://BioRender.com/q80s362).

## DECLARATION OF GENERATIVE AI AND AI-ASSISTED TECHNOLOGIES IN THE WRITING PROCESS

During the preparation of this work, the authors used ChatGPT to refine and improve the English writing. After using this tool/service, the authors reviewed and edited the content as needed and take full responsibility for the content of the publication.

## CRediT AUTHORSHIP CONTRIBUTION STATEMENT

**A. Fosch:** Writing — review & editing, Methodology, Investigation, Data curation. **D.S. Pizarro:** Writing — review & editing, Methodology, Investigation, Data curation. **S. Zagmutt:** Writing — review & editing, Methodology, Data curation. **A.C. Reguera:** Writing — review & editing, Investigation, Data curation. **G. Batallé:** Writing — review & editing, Investigation. **M. Rodríguez-García:** Writing — review & editing, Methodology. **J. García-Chica:** Writing — review & editing, Investigation. **O. Freire-Agulleiro:** Writing — review & editing, Methodology, Investigation. **C. Miralpeix:** Writing — review & editing, Methodology. **P. Zizzari:** Writing — review & editing, Methodology, Investigation. **D. Serra:** Writing — review & editing, Resources, Funding acquisition. **L. Herrero:** Writing — review & editing, Resources, Funding acquisition. **M. López:** Writing — review & editing, Supervision, Resources, Funding acquisition. **D. Cota:** Writing — review & editing, Supervision, Resources, Methodology, Data curation, Conceptualization. **R. Rodríguez-Rodríguez:** Writing — review & editing, Supervision, Resources, Funding acquisition, Formal analysis, Conceptualization. **N. Casals:** Writing — original draft, Supervision, Project administration, Funding acquisition, Conceptualization.

## DECLARATION OF COMPETING INTEREST

The authors declare that they have no known competing financial interests or personal relationships that could have appeared to influence the work reported in this paper.

## DATA AVAILABILITY

Data will be made available on request.

## APPENDIX A. SUPPLEMENTARY DATA

Supplementary data to this article can be found online at https://doi.org/10.1016/j.molmet.2025.102155.

## REFERENCES

[1] Fosch A, Zagmutt S, Casals N, Rodríguez-Rodríguez R. New insights of sf1 neurons in hypothalamic regulation of obesity and diabetes. Int J Mol Sci 2021;22(12). https://doi.org/10.3390/ijms22126186.

[2] Ruffin MP, Nicolaidis S. Electrical stimulation of the ventromedial hypothalamus enhances both fat utilization and metabolic rate that precede and parallel the inhibition of feeding behavior. Brain Res 1999;846(1). https://doi.org/10.1016/S0006-8993(99)01922-8.

[3] Ikeda Y, Luo X, Abbud R, Nilson JH, Parker KL. The nuclear receptor steroidogenic factor 1 is essential for the formation of the ventromedial hypothalamic nucleus. Mol Endocrinol 1995;9(4). https://doi.org/10.1210/mend.9.4.7659091.

[4] Kim KW, Zhao L, Parker KL. Central nervous system-specific knockout of steroidogenic factor 1. Mol Cell Endocrinol 2009. https://doi.org/10.1016/j.mce.2008.09.026.

[5] Kim KW, Zhao L, Donato J, Kohno D, Xu Y, Eliasa CF, et al. Steroidogenic factor 1 directs programs regulating diet-induced thermogenesis and leptin action in the ventral medial hypothalamic nucleus. Proc Natl Acad Sci U S A 2011;108(26). https://doi.org/10.1073/pnas.1102364108.

[6] Zhang J, Chen D, Sweeney P, Yang Y. An excitatory ventromedial hypothalamus to paraventricular thalamus circuit that suppresses food intake. Nat Commun 2020;11(1). https://doi.org/10.1038/s41467-020-20093-4.

[7] Viskaitis P, Irvine EE, Smith MA, Choudhury AI, Alvarez-Curto E, Glegola JA, et al. Modulation of SF1 neuron activity coordinately regulates both feeding behavior and associated emotional states. Cell Rep 2017;21(12). https://doi.org/10.1016/j.celrep.2017.11.089.

[8] Meek TH, Nelson JT, Matsen ME, Dorfman MD, Guyenet SJ, Damian V, et al. Functional identification of a neurocircuit regulating blood glucose. Proc Natl Acad Sci U S A 2016;113(14). https://doi.org/10.1073/pnas.1521160113.

[9] Fosch A, Rodriguez-Garcia M, Miralpeix C, Zagmutt S, Larrañaga M, Reguera AC, et al. Central regulation of brown fat thermogenesis in response to saturated or unsaturated long-chain fatty acids. Int J Mol Sci 2023;24(2). https://doi.org/10.3390/ijms24021697.

[10] Kim KW, Jo YH, Zhao L, Stallings NR, Chua SC, Parker KL. Steroidogenic factor 1 regulates expression of the cannabinoid receptor 1 in the ventromedial hypothalamic nucleus. Mol Endocrinol 2008;22(8). https://doi.org/10.1210/me.2008-0127.

[11] Cardinal P, André C, Quarta C, Bellocchio L, Clark S, Elie M, et al. CB1 cannabinoid receptor in SF1-expressing neurons of the ventromedial hypothalamus determines metabolic responses to diet and leptin. Mol Metabol 2014;3(7). https://doi.org/10.1016/j.molmet.2014.07.004.

[12] Price N, van der Leij F, Jackson V, Corstorphine C, Thomson R, Sorensen A, et al. A novel brain-expressed protein related to carnitine palmitoyltransferase I. Genomics 2002;80(4):433—42.

 

[13] Dai Y, Wolfgang MJ, Cha SH, Lane MD. Localization and effect of ectopic expression of CPT1c in CNS feeding centers. Biochem Biophys Res Commun 2007;359(3):469—74.
[14] Ramírez S, Martins L, Jacas J, Carrasco P, Pozo M, Clotet J, et al. Hypothalamic ceramide levels regulated by CPT1C mediate the orexigenic effect of ghrelin. Diabetes 2013;62(7):2329—37. https://doi.org/10.2337/db12-1451.
[15] Gao S, Zhu G, Gao X, Wu D, Carrasco P, Casals N, et al. Important roles of brain-specific carnitine palmitoyltransferase and ceramide metabolism in leptin hypothalamic control of feeding. Proc Natl Acad Sci U S A 2011;108(23):9691—6.
[16] Rodríguez-Rodríguez R, Miralpeix C, Fosch A, Pozo M, Calderón-Domínguez M, Perpinyà X, et al. CPT1C in the ventromedial nucleus of the hypothalamus is necessary for brown fat thermogenesis activation in obesity. Mol Metabol 2019;19:75—85. https://doi.org/10.1016/j.molmet.2018.10.010.
[17] Okamoto S, Sato T, Tateyama M, Kageyama H, Maejima Y, Nakata M, et al. Activation of AMPK-regulated CRH neurons in the PVH is sufficient and necessary to induce dietary preference for carbohydrate over fat. Cell Rep 2018;22(3):706—21. https://doi.org/10.1016/j.celrep.2017.11.102.
[18] Pozo M, Rodríguez-Rodríguez R, Ramírez S, Seoane-Collazo P, López M, Serra D, et al. Hypothalamic regulation of liver and muscle nutrient partitioning by brain-specific carnitine palmitoyltransferase 1C in Male mice. Endocrinology 2017;158(7):2226—38. https://doi.org/10.1210/en.2017-00151.
[19] Wolfgang MJ, Kurama T, Dai Y, Suwa A, Asaumi M, Matsumoto S, et al. The brain-specific carnitine palmitoyltransferase-1c regulates energy homeostasis. Proc Natl Acad Sci U S A 2006;103(19):7282—7.
[20] Rodríguez-Rodríguez R, Baena M, Zagmutt S, Paraiso WK, Reguera AC, Fadó R, et al. International union of basic and clinical pharmacology: fundamental insights and clinical relevance regarding the carnitine palmitoyltransferase family of enzymes. Pharmacol Rev 2025;77(3):100051. https://doi.org/10.1016/J.PHARMR.2025.100051.
[21] Casals N, Zammit V, Herrero L, Fadó R, Rodríguez-Rodríguez R, Serra D. Carnitine palmitoyltransferase 1C: from cognition to cancer. Prog Lipid Res 2016;61:134—48. https://doi.org/10.1016/j.plipres.2015.11.004.
[22] Casas M, Fadó R, Domínguez JL, Roig A, Kaku M, Chohnan S, et al. Sensing of nutrients by CPT1C controls SAC1 activity to regulate AMPA receptor trafficking. J Cell Biol 2020;219(10). https://doi.org/10.1083/jcb.201912045.
[23] Palomo-Guerrero M, Fadó R, Casas M, Pérez-Montero M, Baena M, Helmer PO, et al. Sensing of nutrients by CPT1C regulates late endosome/lysosome anterograde transport and axon growth. Elife 2019;8. https://doi.org/10.7554/eLife.51063.
[24] Fadó R, Rodríguez-Rodríguez R, Casals N. The return of malonyl-CoA to the brain: cognition and other stories. Prog Lipid Res 2021. https://doi.org/10.1016/j.plipres.2020.101071.
[25] Rodríguez-Rodríguez R, Fosch A, Garcia-Chica J, Zagmutt S, Casals N. Targeting carnitine palmitoyltransferase 1 isoforms in the hypothalamus: a promising strategy to regulate energy balance. J Neuroendocrinol 2023;35(9). https://doi.org/10.1111/jne.13234.
[26] Miralpeix C, Reguera AC, Fosch A, Casas M, Lillo J, Navarro G, et al. Carnitine palmitoyltransferase 1C negatively regulates the endocannabinoid hydrolase ABHD6 in mice, depending on nutritional status. Br J Pharmacol 2021;178(7). https://doi.org/10.1111/bph.15377.
[27] Tokutake Y, Onizawa N, Katoh H, Toyoda A, Chohnan S. Coenzyme A and its thioester pools in fasted and fed rat tissues. Biochem Biophys Res Commun 2010;402(1):158—62. https://doi.org/10.1016/j.bbrc.2010.10.009.
[28] Tokutake Y, Iio W, Onizawa N, Ogata Y, Kohari D, Toyoda A, et al. Effect of diet composition on coenzyme A and its thioester pools in various rat tissues. Biochem Biophys Res Commun 2012;423(4):781—4. https://doi.org/10.1016/j.bbrc.2012.06.037.
[29] Lane MD, Wolfgang M, Cha S-H, Dai Y. Regulation of food intake and energy expenditure by hypothalamic malonyl-CoA. Int J Obes 2008;32(Suppl 4):S49—54. https://doi.org/10.1038/ijo.2008.123.
[30] Hu Z, Cha SH, Chohnan S, Lane MD. Hypothalamic malonyl-CoA as a mediator of feeding behavior. Proc Natl Acad Sci 2003;100(22):12624—9. https://doi.org/10.1073/pnas.1834402100.
[31] Cha SH, Rodgers JT, Puigserver P, Chohnan S, Lane MD. Hypothalamic malonyl-CoA triggers mitochondrial biogenesis and oxidative gene expression in skeletal muscle: role of PGC-1alpha. Proc Natl Acad Sci U S A 2006;103(42):15410—5.
[32] López M, Lelliott CJ, Tovar S, Kimber W, Gallego R, Virtue S, et al. Tamoxifen-induced anorexia is associated with fatty acid synthase inhibition in the ventromedial nucleus of the hypothalamus and accumulation of malonyl-CoA. Diabetes 2006;55(5):1327—36. https://doi.org/10.2337/db05-1356.
[33] Gao L, Chiou W, Tang H, Cheng X, Camp HS, Burns DJ. Simultaneous quantification of malonyl-CoA and several other short-chain acyl-CoAs in animal tissues by ion-pairing reversed-phase HPLC/MS. J Chromatogr B 2007;853(1—2):303—13. https://doi.org/10.1016/j.jchromb.2007.03.029.
[34] He W, Lam TK, Obici S, Rossetti L. Molecular disruption of hypothalamic nutrient sensing induces obesity. Nat Neurosci 2006;9(2):227—33.
[35] López M, Lage R, Saha AK, Pérez-Tilve D, Vázquez MJ, Varela L, et al. Hypothalamic fatty acid metabolism mediates the orexigenic action of ghrelin. Cell Metab 2008;7(5):389—99. https://doi.org/10.1016/j.cmet.2008.03.006.
[36] López M, Varela L, Vázquez MJ, Rodríguez-Cuenca S, González CR, Velagapudi VR, et al. Hypothalamic AMPK and fatty acid metabolism mediate thyroid regulation of energy balance. Nat Med 2010;16(9):1001—8. https://doi.org/10.1038/nm.2207.
[37] Wolfgang MJ, Lane MD. The role of hypothalamic Malonyl-CoA in energy homeostasis. J Biol Chem 2006;281(49):37265—9. https://doi.org/10.1074/jbc.R600016200.
[38] Fadó R, Soto D, Miñano-Molina AJ, Pozo M, Carrasco P, Yefimenko N, et al. Novel regulation of the synthesis of α-Amino-3-hydroxy-5-methyl-4-isoxazolepropionic acid (AMPA) receptor subunit GluA1 by carnitine palmitoyltransferase 1C (CPT1C) in the hippocampus. J Biol Chem 2015;290(42):25548—60. https://doi.org/10.1074/jbc.M115.681064.
[39] Gratacòs-Batlle E, Olivella M, Sánchez-Fernández N, Yefimenko N, Miguez-Cabello F, Fadó R, et al. Mechanisms of CPT1C-Dependent AMPAR trafficking enhancement. Front Mol Neurosci 2018;11:275. https://doi.org/10.3389/fnmol.2018.00275.
[40] Zagmutt S, Mera P, González-García I, Ibeas K, Romero M del M, Obri A, et al. CPT1A in AgRP neurons is required for sex-dependent regulation of feeding and thirst. Biol Sex Differ 2023;14(1). https://doi.org/10.1186/s13293-023-00498-8.
[41] Castellanos-Jankiewicz A, Guzmán-Quevedo O, Fénelon VS, Zizzari P, Quarta C, Bellocchio L, et al. Hypothalamic bile acid-TGR5 signaling protects from obesity. Cell Metab 2021;33(7):1483—1492.e10. https://doi.org/10.1016/J.CMET.2021.04.009.
[42] Miralpeix C, Fosch A, Casas J, Baena M, Herrero L, Serra D, et al. Hypothalamic endocannabinoids inversely correlate with the development of diet-induced obesity in male and female mice. JLR (J Lipid Res) 2019;60(7). https://doi.org/10.1194/jlr.M092742.
[43] Wang H, Eckel RH. Lipoprotein lipase: from gene to obesity. Am J Physiol Endocrinol Metab 2009;297(2). https://doi.org/10.1152/AJPENDO.90920.2008.
[44] Holland J, Sorrell J, Yates E, Smith K, Arbabi S, Arnold M, et al. A brain-melanocortin-vagus axis mediates adipose tissue expansion independently of energy intake. Cell Rep 2019;27(8). https://doi.org/10.1016/j.celrep.2019.04.089.
[45] Nogueiras R, Wiedmer P, Perez-Tilve D, Veyrat-Durebex C, Keogh JM, Sutton GM, et al. The central melanocortin system directly controls peripheral lipid metabolism. J Clin Investig 2007;117(11). https://doi.org/10.1172/JCI31743.
[46] Gao XF, Chen W, Kong XP, Xu AM, Wang ZG, Sweeney G, et al. Enhanced susceptibility of Cpt1c knockout mice to glucose intolerance induced by a high-fat diet involves elevated hepatic gluconeogenesis and decreased skeletal muscle glucose uptake. Diabetologia 2009;52(5):912—20. https://doi.org/10.1007/s00125-009-1284-0.

  

[47] Huang KP, Ronveaux CC, Knotts TA, Rutkowsky JR, Ramsey JJ, Raybould HE. Sex differences in response to short-term high fat diet in mice. Physiol Behav 2020;221. https://doi.org/10.1016/j.physbeh.2020.112894.

[48] Okada T, Mita Y, Sakoda H, Nakazato M. Impaired adaptation of energy intake induces severe obesity in aged mice on a high-fat diet. Physiological Reports 2019;7(3). https://doi.org/10.14814/phy2.13989.

[49] Fabelo C, Hernandez J, Chang R, Seng S, Alicea N, Tian S, et al. Endocannabinoid signaling at hypothalamic steroidogenic factor-1/proopiomelanocortin synapses is sex-and diet-sensitive. Front Mol Neurosci 2018;11. https://doi.org/10.3389/fnmol.2018.00214.

[50] Conde K, Fabelo C, Krause WC, Propst R, Goethel J, Fischer D, et al. Testosterone rapidly augments retrograde endocannabinoid signaling in proopiomelanocortin neurons to suppress glutamatergic input from steroidogenic factor 1 neurons via upregulation of diacylglycerol Lipase-α. Neuroendocrinology 2017;105(4):341—56. https://doi.org/10.1159/000453370.

[51] Rau AR, Hentges ST. Energy state alters regulation of proopiomelanocortin neurons by glutamatergic ventromedial hypothalamus neurons: pre- and postsynaptic mechanisms. J Neurophysiol 2021;125(3):720—30. https://doi.org/10.1152/JN.00359.2020.

[52] Sternson SM, Shepherd GM, Friedman JM. Topographic mapping of VMH –> arcuate nucleus microcircuits and their reorganization by fasting. Nat Neurosci 2005;8(10):1356—63.

[53] Basu R, Elmendorf AJ, Lorentz B, Mahler CA, Lazzaro O, App B, et al. Ventromedial hypothalamic nucleus subset stimulates tissue thermogenesis via preoptic area outputs. Mol Metabol 2024;84. https://doi.org/10.1016/j.molmet.2024.101951.

[54] González-García, I., Milbank, & E., Martinez-Ordoñez, A., Carlos Diéguez, &., López, M., Contreras, C., n.d. HYPOTHesizing about central comBAT against obesity, Doi: 10.1007/s13105-019-00719-y/Published.

[55] Miralpeix C, Reguera AC, Fosch A, Zagmutt S, Casals N, Cota D, et al. Hypothalamic endocannabinoids in obesity: an old story with new challenges. Cell Mol Life Sci 2021. https://doi.org/10.1007/s00018-021-04002-6.

[56] Mazier W, Saucisse N, Gatta-Cherifi B, Cota D. The endocannabinoid system: pivotal orchestrator of obesity and metabolic disease. Trends Endocrinol Metabol 2015;26(10):524—37. https://doi.org/10.1016/j.tem.2015.07.007.

[57] Mazier W, Saucisse N, Simon V, Cannich A, Marsicano G, Massa F, et al. mTORC1 and CB1 receptor signaling regulate excitatory glutamatergic inputs onto the hypothalamic paraventricular nucleus in response to energy availability. Mol Metabol 2019;28:151—9. https://doi.org/10.1016/J.MOLMET.2019.08.005.

[58] Fisette A, Tobin S, Décarie-Spain L, Bouyakdan K, Peyot ML, Madiraju SRM, et al. α/β-Hydrolase domain 6 in the ventromedial hypothalamus controls energy metabolism flexibility. Cell Rep 2016;17(5):1217—26. https://doi.org/10.1016/j.celrep.2016.10.004.

[59] Carrasco P, Sahun I, McDonald J, Ramirez S, Jacas J, Gratacos E, et al. Ceramide levels regulated by carnitine palmitoyltransferase 1C control dendritic spine maturation and cognition. J Biol Chem 2012;287(25):21224—32.

[60] Iborra-Lázaro G, Djebari S, Sánchez-Rodríguez I, Gratacòs-Batlle E, Sánchez-Fernández N, Radošević M, et al. CPT1C is required for synaptic plasticity and oscillatory activity that supports motor, associative and non-associative learning. J Physiol (Paris) 2023;601(16). https://doi.org/10.1113/JP284248.

 